Vehicle detection in remote sensing imagery based on salient information and local shape feature ☆

Xinran Yu[a], Zhenwei Shi[a,b,c,*]

[a]*Image Processing Center, School of Astronautics, Beihang University, Beijing 100191, P.R. China*
[b]*State Key Laboratory of Virtual Reality Technology and Systems, Beihang University, Beijing 100191, P.R. China*
[c]*Beijing Key Laboratory of Digital Media, Beihang University, Beijing 100191, P.R. China*

Abstract

Vehicle detection in high resolution optical imagery, with a variety of civil and military applications, has been widely studied. It is not an easy task since high resolution makes optical imagery complicated, which usually necessitates some rapid predetection methods followed by more accurate processes to accelerate the whole approach and to decrease false alarms. Given this "coarse to fine" strategy, we employ a new method to detect vehicles in remote sensing imagery. First, we convert the original panchromatic image into a "fake" hyperspectral form via a simple transformation, and predetect vehicles using a hyperspectral algorithm. Simple as it is, this transformation captures the salient information of vehicles, enhancing the separation between vehicle and clutter. Then to validate real vehicles from the predetected vehicle candidates, hypotheses for vehicles are generated using AdaBoost algorithm, with Haar-like feature serving as the local feature descriptor. This approach is tested on real optical panchromatic images as well as the simulated images extracted from hyperspectral images. The experiments indicate

☆The work was supported by the National Natural Science Foundation of China under the Grants 61273245 and 91120301, the 973 Program under the Grant 2010CB327904, the Program for New Century Excellent Talents in University of Ministry of Education of China under the Grant NCET-11-0775 and the funding project of State Key Laboratory of Virtual Reality Technology and Systems, Beihang University under the Grant VR-2014-ZZ-02.

*Corresponding author. Tel.: +86-10-823-39-520; Fax: +86-10-823-38-798.
Email address: shizhenwei@buaa.edu.cn (Zhenwei Shi)

that the predetecting method is better than some existing methods such as principal component analysis based algorithm, Bayesian algorithm, etc. The whole process of our approach also performs well on the two types of data.

Keywords: Vehicle Detection, "Reed-Xiaoli" Algorithm, Remote Sensing Imagery Analysis, Haar-like feature, Adaboost Algorithm.

---

1. Introduction

Vehicle detection is of great significance because of its wide applications such as transportation control, road verification, visual surveillance, etc. With the development of sensor technology, high resolution optical images such as GeoEye, QuickBird, Google-Earth are publicly available and become one of the data sources which have been most studied. High resolution images produce more details of vehicles, so the local shape and contextual information are widely used to generate hypotheses separating vehicles from non-vehicle objects. However, higher resolution also makes optical imagery more complicated, which increases the difficulty in detecting vehicles.

In the past two decades, many different approaches have been investigated. These approaches can be roughly divided into two categories: statistics based methods and feature based methods. For the former ones, algorithms such as principal component analysis, Bayesian model as well as threshold segment methods [16] are usually used. As to the latter ones, great attention has been paid to the different kinds of features such as histogram of oriented gradients, local binary patterns, Haar-like features, etc [6]. But in most cases, the existing approaches combine different methods together so as to detect vehicles more efficiently. For example, Leitloff, Hinz and Stilla [10] come up with a sophisticated model of typical traffic situations in urban areas. Firstly, vehicle queues are detected using a line extraction technique, then adaptive boosting algorithm in combination with Haar-like features is employed to separate vehicles out of non-vehicles. Eikvil, Aurdal and Koren [3] employ an automatic approach consisting of a segmentation step followed by two stages of classification to detect vehicles on highways and inner city roads. Choi and Yang [2] utilize Mean-shift algorithm to extract car blobs first and detect cars using log-polar shape descriptor. Cao *et al.* [1] extract the boosted Histogram Orientation Gradients features, followed by a support vector machine to find out vehicles. Kembhavi, Harwood, and Davis [9] propose a vehicle detector including partial least squares algorithm and

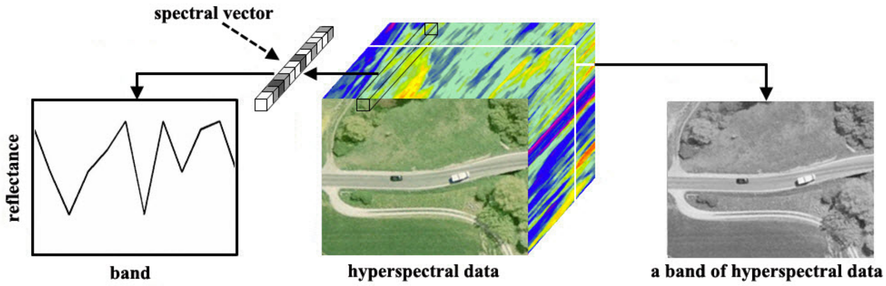

Figure 1: The middle is a hyperspectral image, the left part is the spectral vector of a pixel, and the right part is a single band which is similar to optical image.

a very large set of image descriptors, including color statistics, histograms of oriented gradients as well as a descriptor that captures the structural characteristics of objects.

In this paper, we want to further investigate the problem of vehicle detection in panchromatic remote sensing imagery. Our approach involves a transformation from panchromatic image to a "fake" hyperspectral form. So hyperspectral imagery is introduced briefly here. Hyperspectral image is an image consisting of a set of bands, as Fig. 1 shows. In Fig. 1, each pixel in the hyperspectral image corresponds to a vector named as "spectrum", rather than a single value. The left part of Fig. 1 shows the spectrum of a pixel, which will be denoted as "spectral vector" in the rest of this paper. Some bands in a hyperspectral image may visually be similar to optical image, but others may not. The right part of Fig. 1 shows a certain band. In hyperspectral data, spectral vectors can characterize different kinds of materials since the spectral vectors of different materials usually have different patterns.

Since both spectral vectors of hyperspectral image and the gray values of optical panchromatic image contain discriminative information of different objects, we believe that there could be some underlying relationships between the two types of data. Motivated by this idea, for vehicles in optical panchromatic images, we propose a vehicle detector (or vehicle candidates detector) which detects vehicle candidates in a hyperspectral manner. We first convert the panchromatic image into a "fake" hyperspectral form by transforming neighbored pixels in a panchromatic image into spectral vectors. Then we employ a hyperspectral algorithm to extract vehicles candidates using the

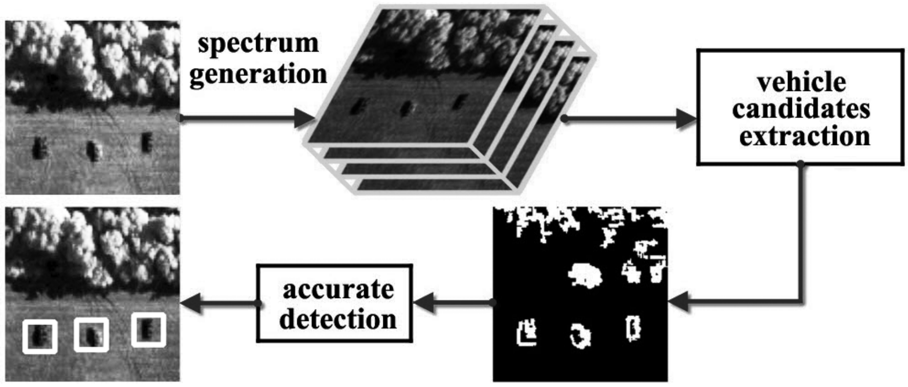

Figure 2: The outline of our method, which can mainly be separated into two parts: Vehicle Candidates Extraction and Accurate Detection.

salient information. Finally, to validate real vehicles from vehicle candidates, hypotheses for vehicles are generated using AdaBoost classifier, with Haar-like feature serving as the local feature descriptor. Fig. 2 presents the outline of our method.

The rest of this paper is organized as follows. Section 2 describes the extraction of vehicle candidates, including the transformation from panchromatic image to "fake" hyperspectral image and the hyperspectral algorithm "Reed-Xiaoli" (RX) [15]. Section 3 briefly depicts the process of Haar-like feature extraction as well as AdaBoost classifier. Section 4 presents the experimental results on real and simulated data. Finally, Section 5 provides the discussion and conclusion of this paper.

2. Vehicle candidates extraction

With the purpose of detecting vehicle candidates preliminarily and quickly, a rapid method to extract all vehicle candidates from the whole image without any omission is needed.

The vehicles in an image are usually more salient than background because the neighbored pixels of vehicles are variable while those of background have great similarities. Then, if we convert the panchromatic imagery into a hyperspectral form, by transforming the neighbored pixels into spectral vectors (defined in section 1), the spectral vectors of vehicles will be very distinct from those of background. Since vehicle pixels usually make up only a small proportion in a whole image, this distinction can be regarded as a kind of anomaly. "Reed-Xiaoli" (RX) algorithm [15], an unsupervised hyperspectral method, can find out the spectral vectors with anomalies and the spectral vectors detected by RX are the vehicle candidates to be further analyzed.

The data produced through the transformation process can be viewed as a kind of "fake" hyperspectral image, i.e., the produced data only has the hyperspectral form but not the hyperspectral information. However, this "fake" hyperspectral imagery can represent data more properly in terms of RX algorithm, which facilitates the subsequent process and analysis. More importantly, through this transformation, the univariate gray level distribution of an one-band image is converted into a multivariate one, enhancing the separability between vehicle and non-vehicle object.

2.0.1. Spectral vector generation

We now explain in details the transformation from a panchromatic image to a "fake" hyperspectral image.

Given an $H \times W$ panchromatic image, a $k \times k$ window is first masked on it and the pixels within the window are copied and shifted into a k^2-dimensional vector, serving as the produced spectral vector. Then the $k \times k$ window traverses throughout the whole image from left to right, from up to bottom and a three-dimensional $H \times W \times k^2$ data cube (ignore the boundary pixels) is finally obtained, as shown in Fig. 3. Note that the $k \times k$ window is the blue square in the left part of Fig. 3 rather than the red sliding window on the right. The red sliding window will be explained later.

2.1. RX algorithm

After generating the "fake" hyperspectral image, the hyperspectral algorithm, "Reed-Xiaoli" (RX), will be explained as we now present. In a produced hyperspectral image, the spectral vector of each pixel can be denoted as a P-dimensional vector of the form $\boldsymbol{x} = (x_1, x_2, ..., x_P)^T$ where $x_i (i = 1, 2, ..., P)$ denotes the value in each band. Then a hyperspectral image with N pixels in total can be denoted as a $P \times N$ matrix $\boldsymbol{X} = [\boldsymbol{x}(1), \boldsymbol{x}(2), ..., \boldsymbol{x}(N)]$ in which each column denotes the spectral vector of each pixel. RX algorithm is capable of detecting the spectral vectors with anomalies which are usually target patterns to be detected among all the N spectral vectors [12].

To be specific, RX algorithm supposes that all spectral vectors in a hyperspectral image are observations from two Gaussian distributions with the same covariance matrix but different mean values. That is to say, the spectral

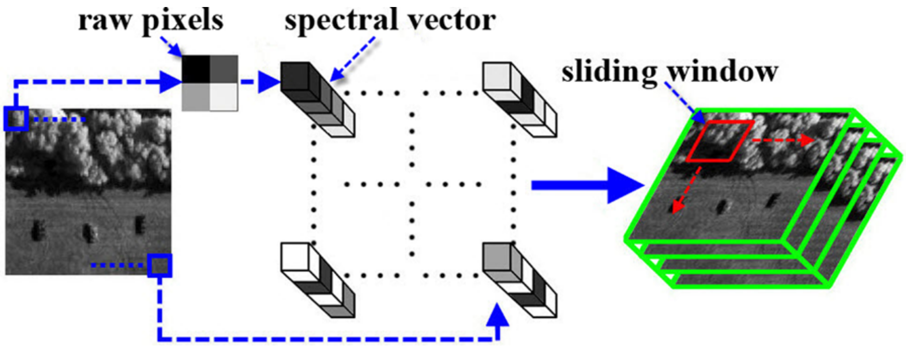

Figure 3: The process of spectral vector generation. The left one is the original image, the right one is the produced hyperspectral form of data with 4-dimensional spectral vectors. The red window is the sliding window.

vectors of background follow $N(\boldsymbol{\mu}_b, \boldsymbol{C}_b)$ and those of target patterns follow $N(\boldsymbol{s}, \boldsymbol{C}_b)$. Given a spectral vector $\boldsymbol{x}(n), n = 1, 2, ..., N$, RX algorithm will distinguish between the two hypotheses below:

$$\begin{aligned} H_0 &: \boldsymbol{x}(n) = \boldsymbol{n} \\ H_1 &: \boldsymbol{x}(n) = \alpha \boldsymbol{s} \end{aligned} \tag{1}$$

for $n = 1, 2, ..., N$, where α is a positive constant, $\boldsymbol{n}$ is a vector denoting background and noise, and $\boldsymbol{s}$ denotes the spectral vector of target patterns. The first hypothesis H_0 models the background as Gaussian distribution $N(\boldsymbol{\mu}_b, \boldsymbol{C}_b)$ and the second hypothesis H_1 models the target patterns as Gaussian distribution $N(\boldsymbol{s}, \boldsymbol{C}_b)$. Notice that $\boldsymbol{\mu}_b$, $\boldsymbol{s}$ and $\boldsymbol{C}_b$ are all unknown but they can be estimated locally or globally from the data.

In order to distinguish the two hypotheses in (1), a measure $\delta_{\mathbf{RX}}(\boldsymbol{x}(n))$ between the spectral vector $\boldsymbol{x}(n)$ and the estimated distribution of background $N(\hat{\boldsymbol{\mu}}_b, \hat{\boldsymbol{C}}_b)$ is computed as the formulae below [13]:

$$\delta_{\mathbf{RX}}(\boldsymbol{x}(n)) = (\boldsymbol{x}(n) - \hat{\boldsymbol{\mu}}_b)^T (\hat{\boldsymbol{C}}_b)^{-1} (\boldsymbol{x}(n) - \hat{\boldsymbol{\mu}}_b) \tag{2}$$

where $\hat{\boldsymbol{C}}_b$ is the maximal likelihood estimated covariance matrix, $\hat{\boldsymbol{\mu}}_b$ is the estimated mean vector:

$$\begin{aligned}\hat{\boldsymbol{C}}_b &= \frac{1}{N}\sum_{n=1}^{N}(\boldsymbol{x}(n) - \hat{\boldsymbol{\mu}}_b)(\boldsymbol{x}(n) - \hat{\boldsymbol{\mu}}_b)^{\mathbf{T}} \\ \hat{\boldsymbol{\mu}}_b &= \frac{1}{N}\sum_{n=1}^{N}\boldsymbol{x}(n)\end{aligned} \tag{3}$$

In fact, $\delta_{\mathbf{RX}}(\boldsymbol{x}(n))$ is the square of the Mahalanobis distance between the spectral vector $\boldsymbol{x}(n)$ and the estimated distribution of background $N(\hat{\boldsymbol{\mu}}_b, \hat{\boldsymbol{C}}_b)$. According to the characteristic of Mahalanobis distance, the spectral vectors which are more salient such as vehicles, shadows and some other clutters will give larger output. Then these pixels can be separated by a threshold which is set automatically by some threshold segment algorithms such as the Otsu's method [14].

2.2. RX algorithm for vehicle detection

In order to apply "Reed-Xiaoli" (RX) algorithm to vehicle detection for panchromatic imagery, some details must be emphasized. The first one is the size of the $k \times k$ patches in the process of spectral vector generation, which has been described in section 2.1. In the rest of this paper, this parameter will be denoted as " sampling range". Sampling range should not be too small, otherwise the "spectral" information will be too little to distinguish the target patterns. And it should not be too large either, otherwise some small targets will be vanished by sampling. The experiments on the size of the sampling range will be shown in Section 4.2.1. After several experiments, the sampling range is finally set to 5×5. That is to say, the "fake" hyperspectral image has $5 \times 5 = 25$ bands.

Another technique must be emphasized is the sliding window. RX is deduced in the condition that the pixels of background follow Gaussian distribution. However, the pixels in the whole image can not satisfy this condition very well due to the complexity of images. Therefore, applying RX to the whole image will be inappropriate and a kind of sliding window will be of great necessity. The sliding window should not be too small. Because the distribution of background is estimated using all the pixels in the whole window, including background and target patterns, as shown in (3). In other words, to estimate background accurately, background must take a large proportion

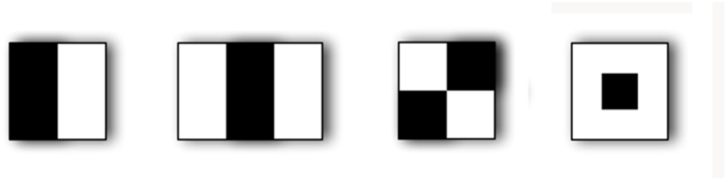

Figure 4: The prototypes used to extract Haar-like features.

while the target patterns a tiny one. From this perspective, the sliding window should be large enough to cover enough background. The experiments on the size of the sliding window will be presented in Section 4.2.2.

The process of spectral vector generation and RX algorithm can be shown in Fig. 3. The left one is the original image, the right one is the produced hyperspectral form of data with 2×2 sampling range, the red window is the sliding window.

3. Accurate detection

After the process of "Reed-Xiaoli" (RX), several false alarms still remain. Our current task is to give a further insight into the extracted vehicle candidates, and to find out vehicles accurately. The AdaBoost classifier [4] trained by Haar-like feature [18] is used.

The purpose of utilizing features rather than raw pixel values is to reduce the intra-class variability while increasing the extra-class one. Meanwhile, feature extraction can also add insensitivity to certain image variations.

Haar-like features are calculated as the sum of pixel values within rectangular regions which are either positive or negative weighted, as shown in Fig. 4, where the white areas are positive weighted and the black ones are negative. According to the special shape of vehicles, four different prototypes are used to extract Haar-like features. The first one is the two-rectangle feature, consisting of two regions with the same size and shape. The two regions are horizontally or vertically adjacent. The second one is the three-rectangle feature, and the sum of the two outside rectangles is subtracted from the sum of the rectangle in the middle. The third one is the four-rectangle feature, which calculates the difference between diagonal pairs of rectangles. Finally, the center feature is computed, by subtracting the center region from the surrounding pixels.

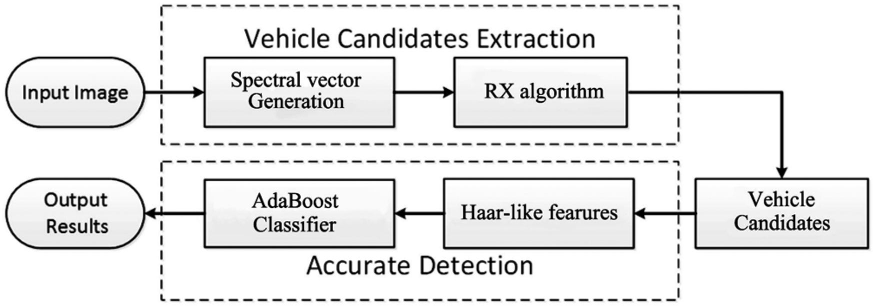

Figure 5: The detailed outline of our method, including spectral vector generation, RX, Haar-like feature extraction and AdaBoost classifier.

After feature extraction, the decision trees trained by AdaBoost algorithm [4] are used to generate hypotheses for vehicles using Haar-like features. AdaBoost algorithm aims at boosting a "weak" learning algorithm or a weak learner which performs just slightly better than random guessing into a arbitrarily accurate "strong" learning algorithm [4]. Specifically, AdaBoost algorithm maintains a distribution or a set of weights over the training set, of which the weights are initialized equally. Then these weights will be updated in T iterations. After T times iterations, the final hypothesis H is a weighted majority vote of the T weak hypotheses. More detailed information can be found in [4].

Thus, the whole process of our method is introduced completely and the detailed outline of our framework is shown in Fig. 5.

4. Experiments results

4.1. Data set

In the experiments, two simulated panchromatic images extracted from hyperspectral images and ten optical panchromatic images are tested. The simulated image is a single band of real hyperspectral data and we normalize the single band to $0 - 255$ to form the simulated image. The hyperspectral data is taken by the hyperspectral digital imagery collection experiment (HYDICE) sensor, which generates 210 bands with the wavelength ranging from 400 nm to 2500 nm and the 48th band with 870 nm wavelength is picked to make the simulated images. The spacial resolution of the simulated images is

Figure 6: The samples of images to be tested. The first row is the single band hyperspectral image and the second row is the panchromatic optical image.

about 1−m. The ten panchromatic images come from Google Earth software and the spacial resolution is about 0.5−m. The simulated panchromatic images are magnified two times by bilinear interpolation so that the vehicles in the two types of data will approximate in size. Fig. 6 shows two images of the two types.

To train the AdaBoost classifier, a database consisting of 781 positive samples and 853 negative samples are used. The vehicles in our images are about 15×10 pixels, in order to cover the vehicles, the positive samples are 30×30 subimages. The negative samples are also 30×30 subimages containing trees, roads, grassland, etc. To detect vehicles of different orientations, the original positive samples are rotated 45 degree for 3 times, and we obtain 4 classifiers to detect vehicles in different orientations.

4.2. Parameters selection

In this section, the experiments on “Reed-Xiaoli” (RX) algorithm are conducted to select proper parameters, i.e. the sampling range and sliding window in the process of spectral vector generation.

4.2.1. Sampling range selection

The sampling range is important to the final results. To evaluate its influence, the sampling range are tested from 3×3 to 15×15. Fig. 7 shows the results of different sampling ranges: 3×3, 5×5, 10×10, 15×15. In Fig. 7, the left column shows two original images, the right columns show the results of "Reed-Xiaoli" (RX) algorithm with different sampling ranges.

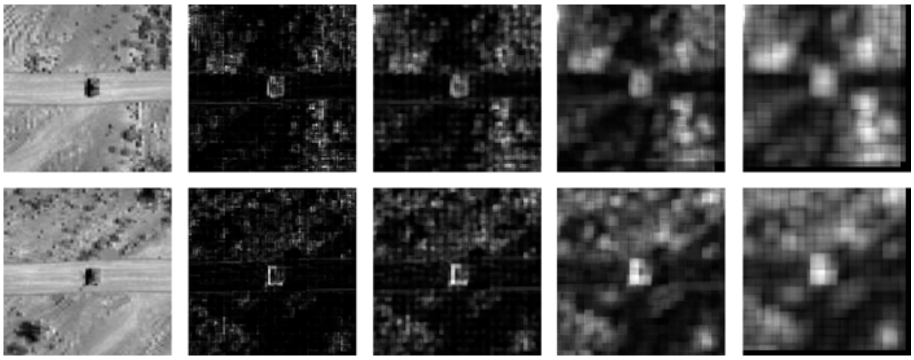

Figure 7: The results of RX with different sampling ranges. The left column shows the two original images, the right columns show the results of RX algorithm with different sampling ranges. The sampling ranges are, from left to right, 3×3, 5×5, 10×10, 15×15.

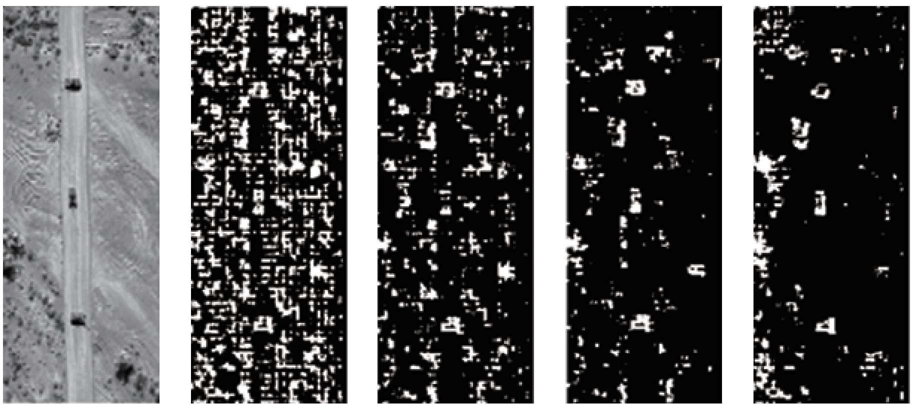

Figure 8: The results of RX with different sliding windows. The first column is the original image, others are the results with different sliding windows. The sliding windows are, from left to right, 20×20, 40×40, 60×60, 100×100.

According to Fig. 7, when the sampling range is 3×3, the vehicles in the middle of the two images can be seen clearly. However, the middle areas of the vehicles tend to be black. The reason is that compared with the size of the vehicles, 3×3 is too small, therefore, the spectral vectors of middle areas of vehicles are relatively smooth, which are similar to those of background. When the sampling range goes up to 5×5, as shown in the third column of Fig. 7, the performance is better. When the sampling range continues to go up, as shown in the fourth and fifth columns, however, the background also gives much larger output. Given the analysis above, the sampling range in our method is set to 5×5.

4.2.2. Sliding window selection

Now we want to test another parameter in the process of spectral vector generation, the size of sliding window. Given the analysis in section 2, the size of sliding window must be selected properly since too large or too small sliding window will violate the assumptions of "Reed-Xiaoli" (RX) algorithm. The size to be tested of sliding window ranges from 20×20 to 100×100. For each sliding window, the output of RX algorithm is processed by a unified threshold (0.12×255) which is set empirically. Thus, the results are all binary images. Fig. 8 shows the results of a 450×178 image.

When the size of sliding window is 20×20, as shown in the second column of Fig. 8, the performance is bad, because too little information is covered. When the size of sliding window increases, the performance becomes much better. Given the results in Fig. 8, the sliding window in our method is set to 60×60.

4.3. Evaluation of RX algorithm

To further test the performance of "Reed-Xiaoli" (RX), this algorithm is compared with four other existing methods, i.e. principal component analysis (PCA), Bayesian background transformation (BBT), gradient threshold (GT), and morphological method. The first three are studied in [16], and the last one is proposed in [19]. For GT and the morphological method, whose thresholds are fixed, their results of a 915×178 image are given in Fig. 9. As to PCA and BBT, their results are given in the form of receiver operating characteristic curve or ROC curve, as shown in Fig. 10. Its X-axis and Y-axis are calculated by the formulae below. Notice that the ground-truth is produced manually.

$$\begin{aligned} \text{True positive rate} &= \frac{\text{Positives correctly classified}}{\text{Total positives}} \\ \text{False positive rate} &= \frac{\text{Negatives incorrectly classified}}{\text{Total negatives}} \end{aligned} \tag{4}$$

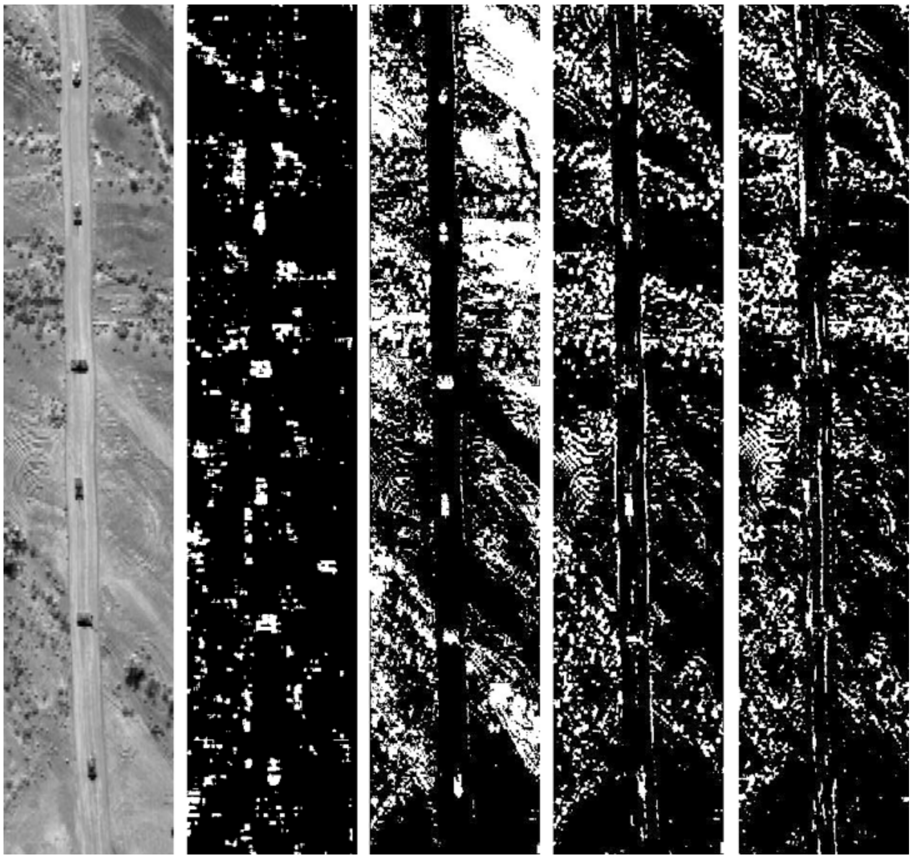

Figure 9: The results of RX, GT and the morphological method. The first column is the original image, the second column is the result of RX, the third column is the result of GT and the last two columns are the results of morphological opening and closing based methods.

According to Fig. 9, RX algorithm performs better than GT and morphological method. For RX, all the six vehicles are detected and the false alarms are less than GT and morphological method. From the second column of Fig. 9, it can be seen that the smooth area like road can be eliminated. Compared with the threshold methods which focus on the gray values, RX algorithm concerns more on the salient information of an image. In other words, the pixels which are greatly distinct from their neighborhoods will be enhanced, while others will be suppressed. Therefore, vehicles as well as some other clutters will be detected.

Fig. 10 presents the ROC curves of RX, PCA and BBT. ROC curves

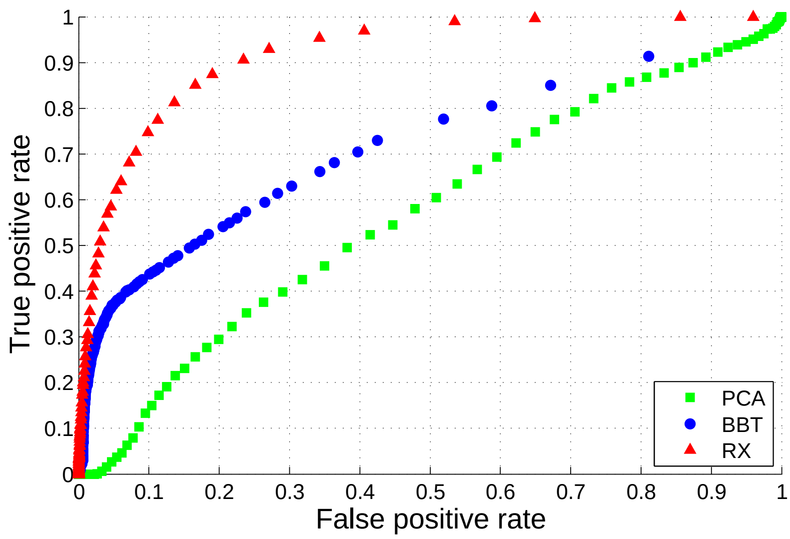

Figure 10: The ROC curves of RX, BBT and PCA.

depict the relative tradeoffs between benefits (true positives) and costs (false positives). The curve in the upper-left region of the graph is best and it can be seen from Fig. 10 that RX is better than PCA and BBT. In fact, the advantage of RX over PCA and BBT could lie in the produced spectral vectors, which expand the univariate gray level distribution of an image to a multivariate one. Although the produced bands all come from the original image, and these bands are high related from a global perspective, however, from a local perspective, these spectral vectors increase the separability between salient and smooth areas. Besides, through this transformation, contextual information is imported into RX algorithm, which leads to better performance.

4.3.1. RX for urban scene

RX is also tested in urban scene, in which the background is usually more complex. Fig. 11 shows the results of an urban scene. It can be seen from Fig. 11(b) that the result of RX has many false alarms, but some extracted areas are either too small or too large to be a vehicle. So the size, length and length-width ratio of the connected areas are analyzed and the unreasonably sized areas are filtered. Fig. 11(c) shows the result after

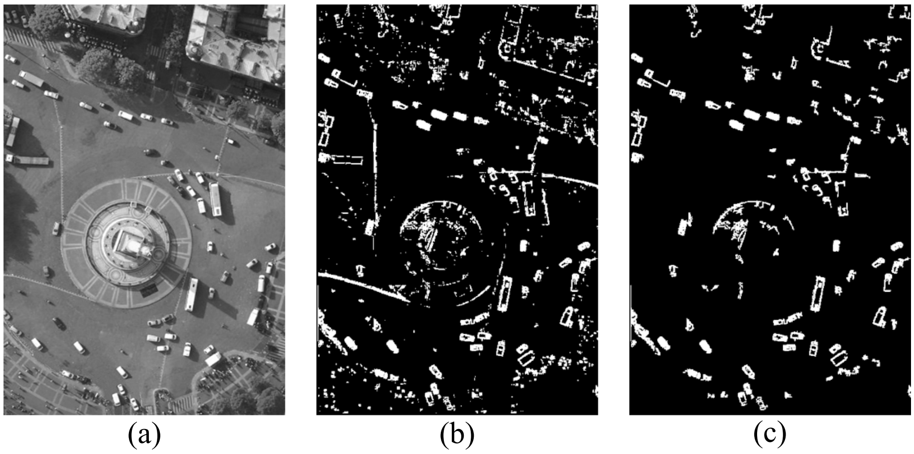

Figure 11: The result of RX of urban scene, (a) is the panchromatic image, (b) is the result of RX and (c) is the result after removing unreasonably sized areas.

Table 1: The Results of AdaBoost Classifier with and without RX

Methods	detection rate(%)	false alarm rate(%)	processing time(s)
Adaboost without RX	96.3	12.6	143.9
Adaboost with RX	**95.4**	**4.8**	**26.4**

removing unreasonably sized areas. It can be seen from Fig. 11 that when the background is more complex, RX can still remove large areas of smooth background.

4.4. Evaluation of the whole process

In this section, we want to test the whole process of our approach. Table 1 shows the results of our approach with and without "Reed-Xiaoli" (RX) algorithm. As Table 1 shows, with the implement of RX, the detection rate is decreased by about 1%, but the false alarm rate is reduced by almost 8%. In addition, RX reduces the whole processing time from 143.9s to 26.4s.

4.4.1. Simulated image experiments

Fig. 12 shows the final results of the two simulated images extracted from the hyperspectral images. The first one shows a desert region with six

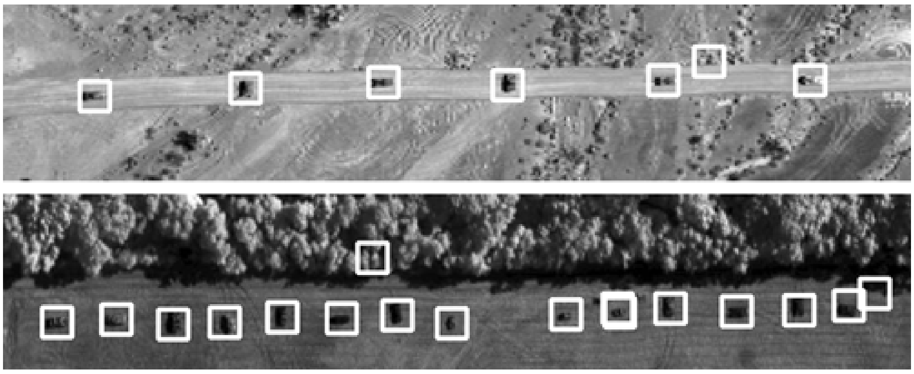

Figure 12: The results in 48th band hyperspectral image, the white squares denote the vehicles detected.

vehicles along the road and the second one is a forest area with fourteen vehicles near the trees. It can be seen in Fig. 12 that all the vehicles are detected but some false alarms still remain.

4.4.2. Optical panchromatic image experiments

Fig. 13 shows the results of our approach on optical panchromatic images. In Fig. 13 (a)-(d), the vehicles are on the road or on the bridge and the background includes trees, shadows, grass land, road marking. In Fig. 13(e), the vehicles are in an urban scene with more complicated background clutters such as buildings, road markings, etc. obviously, the background clutters of the optical images are much more complicated than those of the simulated images. As Fig. 13 shows, although the complexity increases, all vehicles are detected by our approach. The false alarms still exist, but the false alarms rate is in a low level.

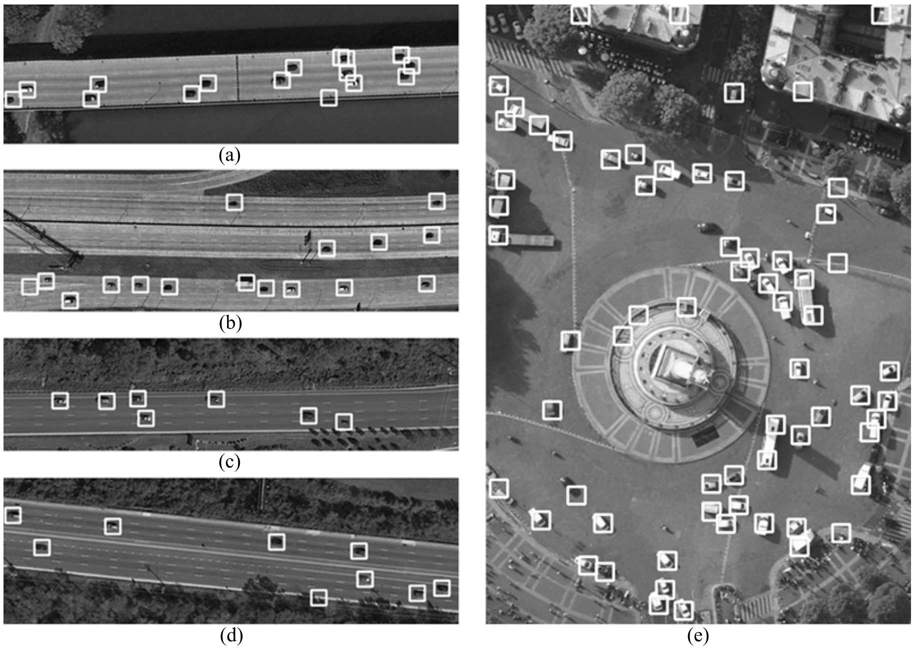

Figure 13: The results in optical images from Google-Earth, the white squares denote the vehicles detected.

5. Conclusions

In this paper, we propose a new method to detect vehicles in panchromatic remote sensing imagery and introduce a hyperspectral algorithm to the optical detection domain. We first transform the one-band image into a "fake" hyperspectral form, expand the univariate gray level distribution of one-band image into a multivariate one, and extract vehicle candidates preliminarily and quickly using "Reed-Xiaoli" (RX) algorithm. Through this transformation, the contextual information of vehicles are collected, making more discriminative information available for RX, enhancing the separability between vehicles and background. Then to validate real vehicles out of vehicle candidates, hypotheses for vehicles are generated using AdaBoost algorithm and Haar-like features. This method shows good performance and robustness in experiments on simulated images as well as real panchromatic images from Google-Earth.

References

[1] X. Cao, C. Wu and P. Yan. Linear SVM classification using boosting HOG features for vehicle detection in low-altitude airborne videos. International Conference on Image Processing (ICIP)(2011), pp. 2421-2424.

[2] J. Y. Choi and Y. K. Yang. Vehicle detection from aerial images using local shape information. Advances in Image and Video Technology, (2009), pp. 227-236.

[3] L. Eikvil, L. Aurdal and H. Koren. Classification-based vehicle detection in high-resolution satellite images. ISPRS J. Photogram. Remote Sens., 64(1)(2009), pp. 65-72.

[4] Y. Freund and R. Schapire. A desicion-theoretic generalization of on-line learning and an application to boosting. Computational learning theory, (1995), pp. 23-37.

[5] A. Gerhardinger, D. Ehrlich and M. Pesaresi. Vehicle detection from very high resolution satellite imagery for the development of a social activity index. International Archives of Photogrammetry, Remote Sensing and Spatial Information Sciences (2005), pp. 83-88.

[6] H. Grabner, T. T. Nguyen and B. Gruber. On-line boosting-based car detection from aerial images. ISPRS, J. Photogram. Remote Sens., 63(3)(2008), pp. 382-396.

[7] S. Hinz and U. Stilla. Car detection in aerial thermal images by local and global evidence accumulation. Pattern recognition letters, 27(4)(2006), pp. 308-315.

[8] X. Jin and C. H. Davis. Vehicle detection from high-resolution satellite imagery using morphological shared-weight neural networks. Image and Vision Computing, 25(9)(2007), pp. 1422-1431.

[9] A. Kembhavi, D. Harwood and L. S. Davis. Vehicle detection using partial least squares. IEEE Trans. Pattern Anal. Mach. Intell., 33(6)(2011), pp. 1250-1265.

[10] J. Leitloff, S. Hinz and U. Stilla. Vehicle detection in very high resolution satellite images of city areas. IEEE Trans. Geosci. Remote Sens., 48(7)(2010), pp. 2795-2806.

[11] D. Manolakis, D. Marden and G. A. Shaw. Hyperspectral image processing for automatic target detection applications. Lincoln Laboratory Journal, 14(1)(2003), pp. 79-116.

[12] S. Matteoli, M. Diani and G. Corsini. A tutorial overview of anomaly detection in hyperspectral images. IEEE Aerosp. Electron. Syst. Mag., 25(7)(2010), pp. 5-28.

[13] N. M. Nasrabadi. Regularization for spectral matched filter and RX anomaly detector. Proc. SPIE Int. Soc. Opt. Eng., (2008).

[14] N. Otsu. A threshold selection method from gray-level histograms. Automatica, 11(1975), pp. 23-27.

[15] I. S. Reed and X. Yu. Adaptive multiple-band CFAR detection of an optical pattern with unknown spectral distribution. IEEE Trans. Acoust. Speech. Signal Process., 38(10)(1990), pp. 1760-1770.

[16] G. Sharma, C. J. Merry and P. Goel. Vehicle detection in $1-m$ resolution satellite and airborne imagery. Int. J. Remote Sens., 27(4)(2006), pp. 779-797.

[17] M. Shimoni, G. Tolt and C. Perneel. Detection of vehicles in shadow areas. 2011 3rd Workshop on Hyperspectral Image and Signal Processing: Evolution in Remote Sensing (WHISPERS)(2011), pp. 1-4.

[18] P. Viola and M. Jones. Rapid object detection using a boosted cascade of simple features. IEEE Computer Society Conference on Computer Vision and Pattern Recognition (CVPR)(2001), pp. 511-518.

[19] Z. Zheng, X. Wang and G. Zhou. Vehicle detection based on morphology from highway aerial images. IEEE International Geoscience and Remote Sensing Symposium (IGARSS)(2012), pp. 5997-6000.